Surface plasmon resonance assisted rapid laser joining of glass

Svetlana A. Zolotovskaya,[1] Guang Tang,[1] Zengbo Wang,[2] and Amin Abdolvand[1,a)]
[1]School of Engineering, Physics and Mathematics, University of Dundee, Dundee DD1 4HN, United Kingdom
[2]School of Electronic Engineering, Bangor University, Bangor LL57 1UT, United Kingdom

(Received 14 July 2014; accepted 16 August 2014; published online 26 August 2014)

Rapid and strong joining of clear glass to glass containing randomly distributed embedded spherical silver nanoparticles upon nanosecond pulsed laser irradiation (~40 ns and repetition rate of 100 kHz) at 532 nm is demonstrated. The embedded silver nanoparticles were ~30–40 nm in diameter, contained in a thin surface layer of ~10 μm. A joint strength of 12.5 MPa was achieved for a laser fluence of only ~0.13 J/cm^2 and scanning speed of 10 mm/s. The bonding mechanism is discussed in terms of absorption of the laser energy by nanoparticles and the transfer of the accumulated localised heat to the surrounding glass leading to the local melting and formation of a strong bond. The presented technique is scalable and overcomes a number of serious challenges for a widespread adoption of laser-assisted rapid joining of glass substrates, enabling applications in the manufacture of microelectronic devices, sensors, micro-fluidic, and medical devices. © *2014 AIP Publishing LLC*. [http://dx.doi.org/10.1063/1.4894118]

The latest social and environmental developments lead to a much higher electrification and miniaturization of our everyday lives. Industries in the precision machinery, electrical, and healthcare sectors require the development of improved micro-joining/welding techniques. Traditionally, joining techniques, such as adhesive bonding, arc bonding, anodic bonding, and soldering, have been employed for the manufacture of micro-optical, mechanical, electronic, and fluidic devices. In this context, laser micro-joining proved to be a superior method due to its advantages of high speed, high precision, consistent weld intensity, and low heat distortion.[1] In particular, direct joining techniques of glass with a focused ultra-short (femtosecond) pulsed laser beam have recently been reported.[2–8] In these studies, by focusing the ultra-short laser pulses at the interface between the glass substrates, the nonlinear absorption of the beam has been exploited and glass joint strength of 14.9 MPa was reported.[4] However, there are a number of shortcomings associated with this technique. The process requires a lens objective of high numerical aperture, typically in the range of 0.4–0.65. This leads to a poor working distance and welding depth, and ultimately restricts the welding efficiency and the processing speed. It also imposes strict requirements on the surface quality of the work pieces—currently within $\lambda/4$. The above constitutes a serious challenge for widespread adoption of this technique by industry.

In this letter, we report on a scalable and rapid technique for joining clear glass to glass containing randomly distributed embedded spherical silver nanoparticles, also known as metal-glass nanocomposite (MGN). The employed laser is an industrially adaptable source and the presented technique will find applications in sensor and medical device fabrication. We also present a model for the process, which fully supports the observed results and mechanism. According to the model, the absorption of the laser beam by the randomly distributed embedded metallic nanoparticles and expansion of the glass within the nanoparticle-containing layer upon laser irradiation is of paramount importance for the process.

The clear glass samples were commercial Schott B270 white (composition in wt. %: 69.2 SiO_2, 9.8 Na_2O, 9.5 CaO, 7.6 K_2O, 2.8 BaO, 1.1 Al_2O_3, transition temperature of ~530 °C, fire polished surface) and with thicknesses of 1 mm and 4 mm.

The MGN wafers were fabricated from a 1 mm thick soda-lime float glass (comprising in wt. %: 72.5 SiO_2, 14.4 Na_2O, 6.1 CaO, 0.7 K_2O, 4.0 MgO, 1.5 Al_2O_3, 0.1 Fe_2O_3, 0.1 MnO, 0.4 SO_3—transition temperature in the range from 550 to 580 °C, fire polished surface) by Ag^+-Na^+ ion exchange and subsequent annealing at 400 °C in a H_2 reduction atmosphere.[9] This resulted in the formation of randomly distributed spherical silver nanoparticles of ~30–40 nm mean diameter in a thin surface layer of ~10 μm on both sides of the glass substrate. The nanoparticle-containing layers were formed ~30 nm beneath the surface of the glass.[10–12] Single-sided samples were used in our experiments and were made by removing a ~20 μm thick layer from one side of the MGN wafers by etching in 12% HF acid. The extinction spectrum of a typical MGN wafer used in our experiments is shown in Fig. 1(a). The surface plasmon resonance band is peaked at ~430 nm. The optical transmittance of a single-sided MGN wafer is ~63% at 532 nm.

The laser joining of the 15 mm × 12 mm clear glass samples and MGN wafers was performed by utilizing a Nd:YVO_4 laser with a maximum average power of 10 W at $\lambda = 532$ nm with a pulse length of $\tau = 38$ ns and a repetition rate of $f = 100$ kHz. The schematic of the experimental setup is depicted in Fig. 1(b). The laser beam had a Gaussian intensity profile ($M^2 < 1.3$) and was focused onto the interface between the transparent glass samples and MGN wafers using a flat-field scanning lens system (F-theta lens) with a focal length of 160 mm. The diameter of the focused spot was ~60 μm at the $1/e^2$ level.

The samples were irradiated at different scanning speeds (v) with the number of pulses fired per spot (N) varying from 5 to 3000, and laser fluences (F) ranging from 0.03 to 0.70 J/cm^2,

a)Author to whom correspondence should be addressed. Electronic mail: a.abdolvand@dundee.ac.uk

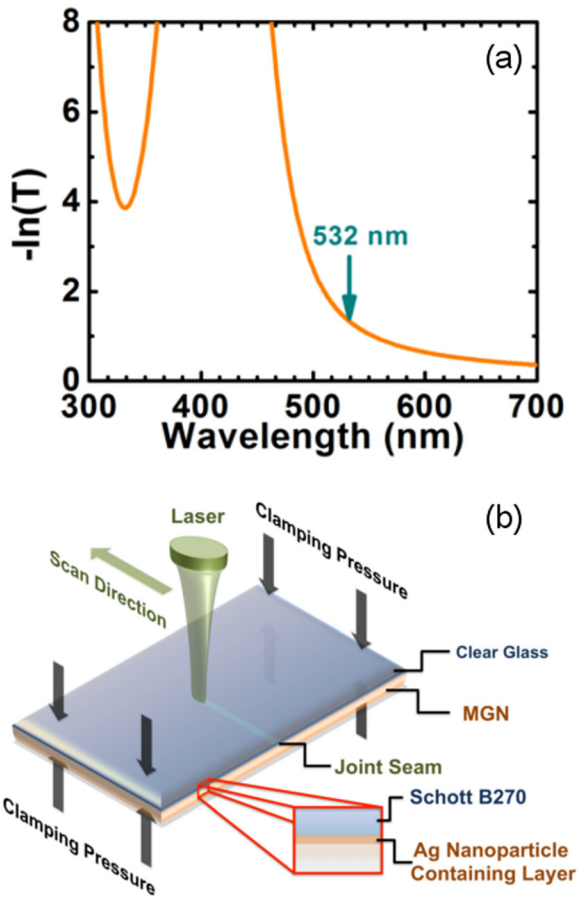

FIG. 1. (a) Extinction spectrum of a typical MGN wafer used in the experiments. (b) Schematic of the experimental set-up for surface plasmon resonance assisted laser joining. The clear glass sample is Schott B270.

taking into account the Fresnel loss at the top transparent glass wafer. A fairly moderate pressure was applied in order to bring the clear glass and MGN wafers in close proximity for laser irradiation. The air gap, estimated from the interference pattern observed after mounting the samples in a mechanical fixture, was ~150 nm. The samples for laser joining were used as received without any additional polishing of the surfaces. Before laser processing, surfaces were cleaned with acetone, propanol then rinsed with deionised water, and dried with a nitrogen gun. The samples were characterised using a spectrophotometer (JASCO V-670) and a Digital Microscope (KEYENCE VHX-1000).

A single line laser irradiation was conducted in order to determine the optimal bonding conditions. At energy fluences below 0.10 J/cm^2 (at fixed $v = 10$ mm/s), the interfacial bonding strength was insufficient to hold the wafers together. For the laser fluences exceeding values of 0.21 J/cm^2, formation of cracks originating at the MGN surface was observed. Using a number of pulses per spot of less than 120 (at fixed $F = 0.13$ J/cm^2) led to a significant reduction in the bonding strength, whilst generation of cracks was observed above $N = 1500$.

An example of multi-line laser joining is shown in Fig. 2(a). A circular-shaped joining contour with an outer diameter of 6 mm and a distance between consecutive scans (T) of 100 μm was achieved at $F = 0.13$ J/cm^2 and $v = 10$ mm/s leading to a set of continuous joining seams of ~42 μm width (t)—inset in Fig. 2(a). No crack formation or heat affected zone were observed. The joint strength was measured to be ~12.5 MPa, utilizing the tensile test procedure described in Ref. 2. The samples separated as a result of the test demonstrated brittle fracture, which verifies the fused joint. A cross section of multi-line laser joining is presented in Fig. 2(b). The joining seam morphology—inset in Fig. 2(b)—reveals that the nanoparticle-containing layer facilitates localized deposition of the laser energy and reduces the energy density levels required for laser joining. The heat affected zone is negligible and is confined to the very interfacial layer in the contact zone. This confirms a low thermal load exerted on the joined components. Furthermore, the multi-line surface plasmon resonance assisted laser joining was applied to hermetically seal a 4 mm × 4 mm region. Figure 3(a) shows the square sealing of the wafers before and after immersion in water. The interference fringes appear to be diminished after immersion while the sealed region is left intact. The possibility of surface plasmon resonance assisted laser joining 3-D components was demonstrated using a 4-mm thick clear glass sample and is presented in Fig. 3(b).

In order to understand the joining mechanism, theoretical calculations based on a coupled electromagnetic (EM)—thermal model have been performed using a commercially available package, details of which can be found elsewhere.[13] Essentially, the model first calculated the optical near-field intensity distributions of the composite system using a 3-D full EM solver. The results were then fed into a transient thermal model, as heating source, to identify the

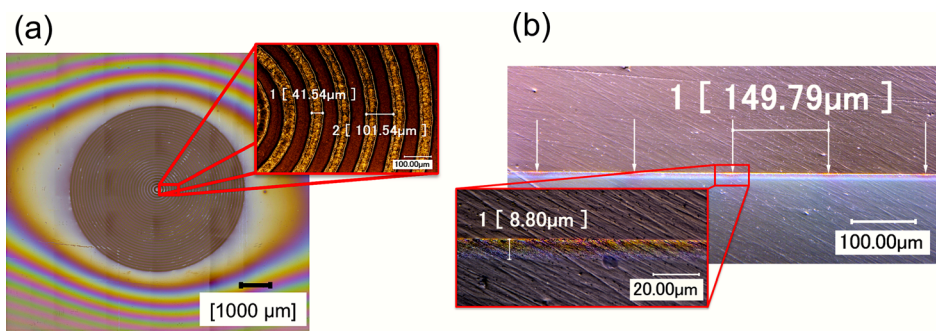

FIG. 2. (a) Circular-shaped multi-line joining contour with an outer diameter of 6 mm. Inset shows the joining seams: $t = 41.5$ μm, $T = 101.5$ μm (bright field image at 500×). (b) Cross-section of a multi-line joint (at 500×): the seams are indicated by white arrows. Inset is the joining seam morphology (at 3000×). The *silver* nanoparticle containing layer of 8.8 μm is clearly resolved. The processing parameters are $F = 0.12$ J/cm^2, $v = 10$ mm/s, and $N = 600$.

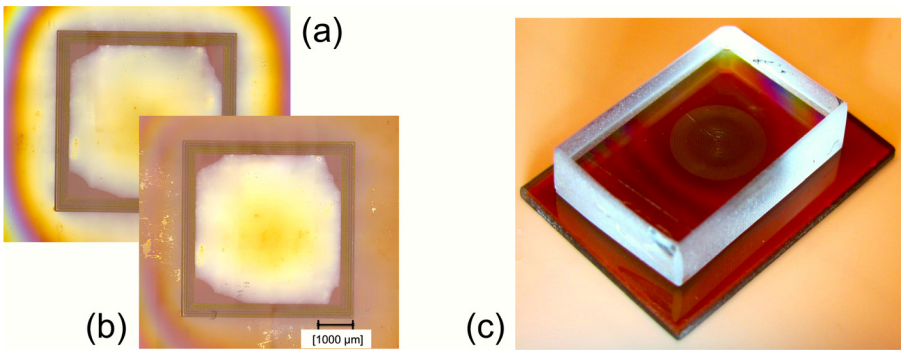

FIG. 3. Hermetic sealing achieved with the multi-line laser joining: bonded wafers before (a) and after (b) immersion in water. (c) Example the surface plasmon resonance assisted joining of 4-mm clear glass—Schott B270 (top) to MGN substrate (bottom).

temperature field evolution of the system. Particular attention was paid to the interfacial regions where the micro-welding process took place. Figure 4 shows the simulated optical and temperature field distributions for *two* extreme representative configurations: specifically, a 2-D regular array with neighbor-particle spacing of (a) 200 nm and (b) 5 nm. The laser parameters for the modeling strictly followed the experiments: laser fluence = 0.13 J/cm^2, pulse duration = 38 ns, glass refractive index $n_g = 1.5$, and silver refractive index $n_{Ag} = 0.13 + 3.1i$.[14]

These results demonstrate that the strong near-field coupling of the multiple silver nanoparticles lead to a significant amplification of the optical fields inside the MGN substrate. For example, at the spacing of 5 nm the field was enhanced by a factor of 350. Such strong field enhancement effect has already found applications in, e.g., surface enhancement Raman Scattering and biomedical sensing. In the present case, these highly localized near-fields serve as highly efficient local heating sources inside the substrate. Given that the MGN wafer contains randomly distributed silver nanoparticles in its doped region and although the nanoparticles are all 30–40 nm in diameter, the particles' spacings are not fixed and vary within a range, typically from few nanometers to 200 nm as estimated from the volume filling factor of the MGN sample. This randomness makes the simulation process rather complex and beyond the scope of the present study. Nevertheless, results presented in Fig. 4 for periodical 2-D array samples are still valid for illustration of the basic

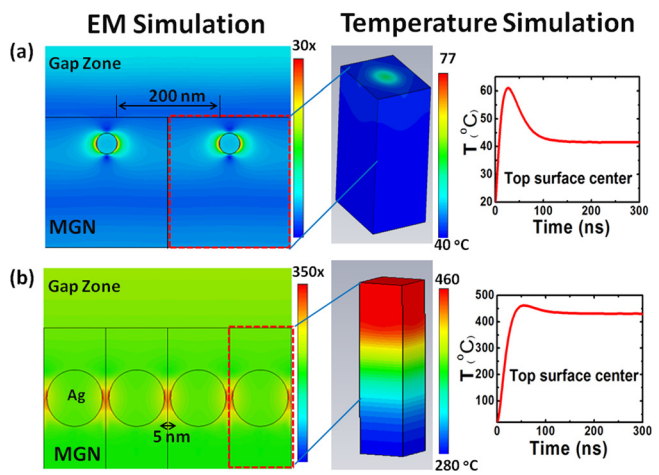

FIG. 4. Simulated optical and temperature field distributions for a 2-D regular array of *silver* nanoparticles, with periodic spacing of (a) 200 nm and (b) 5 nm. As can be seen, the temperature field increases significantly when particles get closer than 10 nm in spacing.

joining mechanism encountered in our work. Part of the delivered laser energy is absorbed and scattered by the nanoparticles while the rest is dissipated into heat. There will be a large number of nanoscale heating sources within each laser spot since multiple nanoparticles are illuminated and heated simultaneously. These heated particles will undergo a complex thermal exchange rebalance process, through conduction, and are responsible for the bonding effects that we observed in the experiments. The temperature range of the MGN sample under laser heating (at fluence 0.13 J/cm^2) is of the order of 60–70 °C for *loosely* neighbored nanoparticles (Fig. 4(a)), and about 400–500 °C for *closely* positioned particles (Fig. 4(b)). Further calculations on the time history of the temperature fields (for the 200 nm-spacing sample) reveal that the heat accumulation effect does indeed exist in our process: at 10 μs (corresponding to the laser repetition rate of $f = 100$ kHz) during the time when the second laser pulse arrives, the MGN surface temperature does not drop back to room temperature (20 °C) but remains at about 36 °C. For complete cooling, it takes about 38 μs, roughly a factor of 10^3 longer than the laser pulse duration of $\tau = 38$ ns. Thus, the heat accumulation effect is indeed essential for building up a sufficient level of thermal energy that melts the two joining glass surfaces. Hence, in order to build up the temperature fields for melting and thus welding (>570 °C), multiple pulses are required. This is in agreement with our experimental observations where about $N = 600$ pulses were required for achieving a good quality joint. We should like to point out that the melting is relatively gentle in our process leading to a strong joint with excellent quality.

In summary, a facile and rapid laser technique for micro-joining of dielectrics was presented. The report comprises rapid mico-bonding of a 1-mm thick soda-lime glass with embedded spherical silver nanoparticles (~30–40 nm in diameter) to a 1-mm thick Schott B270 glass upon nanosecond pulsed laser irradiation at 532 nm at moderate laser energy fluences and clamping pressure. A joint strength of 12.5 MPa was achieved. The welding mechanism was discussed in terms of localised absorption and accumulation of the laser energy by the metallic nanoparticles and the transfer of heat to the surrounding glass leading to the melting and expansion of the substrates and formation of a strong bond.

Here, the employed laser is an industrially adaptable source and the presented technique will find applications in sensor and medical device fabrication. Our future work will aim at investigation into increasing the bond area, joint

strength and reliability of the technique. Our laser welding technique can be extended to joining dissimilar materials with glass and has the potential for various micro-packages applications, such as microfluidic devices, and microelectronic devices.

This work was conducted under the aegis of the Engineering and Physical Sciences Research Council (EPSRC) of the United Kingdom (EP/I004173/1). The support of CODIXX AG is gratefully acknowledged. Amin Abdolvand is an EPSRC Career Acceleration Fellow at the University of Dundee.

[1]A. W. Y. Tan and F. E. H. Tay, "Localized laser assisted eutectic bonding of quartz and silicon by Nd:YAG pulsed-laser," Sens. Actuators, A **120**, 550 (2005).
[2]W. Watanabe, S. Onda, T. Tamaki, K. Itoh, and J. Nishii, "Space-selective laser joining of dissimilar transparent materials using femtosecond laser pulses," Appl. Phys. Lett. **89**, 021106 (2006).
[3]T. Tamaki, W. Watanabe, and K. Itoh, "Laser micro-welding of transparent materials by a localized heat accumulation effect using a femtosecond fiber laser at 1558 nm," Opt. Express **14**, 10460 (2006).
[4]W. Watanabe, S. Onda, T. Tamaki, and K. Itoh, "Direct joining of glass substrates by 1 kHz femtosecond laser pulses," Appl. Phys. B **87**, 85 (2007).
[5]I. Miyamoto, A. Horn, J. Gottmann, D. Wortmann, and F. Yoshino, "Fusion welding of glass using femtosecond laser pulses with high-repetition rates," J. Laser Micro/Nanoeng. **2**(1), 57 (2007).
[6]H. Huang, L. Yang, and J. Liu, "Direct welding of fused silica with femtosecond fiber laser," Proc. SPIE **8244**, 824401 (2012).
[7]W. Watanabe, "Direct joining and welding with ultrashort laser pulses," in *CLEO: 2013* (Optical Society of America, 2013), paper ATu2N.3.
[8]C. Luo and L. Lin, "The application of nanosecond-pulsed laser welding technology in MEMS packaging with a shadow mask," Sens. Actuators, A **97–98**, 398 (2002).
[9]K.-J. Berg, A. Berger, and H. Hofmeister, "Small silver particle in glass-surface layers produced by sodium-silver ion-exchange—their concentration and size depth profile," Z. Phys. D **20**, 309 (1991).
[10]M. A. Tyrk, W. A. Gillespie, G. Seifert, and A. Abdolvand, "Picosecond pulsed laser induced optical dichroism in glass with embedded metallic nanoparticles," Opt. Express **21**, 21823 (2013).
[11]L. A. H. Fleming, S. Wackerow, A. C. Hourd, W. A. Gillespie, G. Seifert, and A. Abdolvand, "Diffractive optical element embedded in silver-doped nanocomposite glass," Opt. Express **20**, 22579 (2013).
[12]L. A. H. Fleming, G. Tang, S. A. Zolotovskaya, and A. Abdolvand, "Controlled modification of optical and structural properties of glass with embedded silver nanoparticles by nanosecond pulsed laser irradiation," Opt. Mater. Express **4**, 969 (2014).
[13]L. Yue, Z. B. Wang, and L. Li, "Multiphysics modelling and simulation of dry laser cleaning of micro-slots with particle contaminants," J. Phys. D: Appl. Phys. **45**, 135401 (2012).
[14]E. D. Palik, *Handbook of Optical Constants of Solids III* (Academic Press, New York, 1998).